

Local Compliance Effects on the Global Pressure-Volume Relationship In Models of Intracranial Pressure Dynamics

S.A. STEVENS* AND W.D. LAKIN†

ABSTRACT

The experimentally-measured pressure-volume relationship for the human intracranial system is a nonlinear “S-shaped” curve with two pressure plateaus, a point of inflection, and a vertical asymptote at high pressures where all capacity for volume compensation is lost. In lumped-parameter mathematical models of the intracranial system, local compliance parameters relate volume adjustments to dynamic changes in pressure differences between adjacent model subunits. This work explores the relationship between the forms used for local model compliances and the calculated global pressure-volume relationship. It is shown that the experimentally-measured global relationship can be recovered using physiologically motivated expressions for the local compliances at the interfaces between the venous-cerebrospinal fluid (CSF) subunits and arterial-CSF subunits in the model. Establishment of a consistent link between local model compliances and the physiological bulk pressure-volume relationship is essential if lumped-parameter models are to be capable of realistically predicting intracranial pressure dynamics.

Key words: • cerebrospinal fluid (CSF) • lumped-parameter models • compliances • dynamic intracranial pressures

1 INTRODUCTION

Lumped-parameter models provide an attractive means of studying dynamic processes in the intracranial system. In this modeling approach, fluid and matter constituents of the dynamic system are subdivided into a number of interacting subunits. Consistent with earlier work on intracranial pressure using this type of model [10, 21], each model subunit will be termed a “compartment.” A single physical constituent, e. g. brain matter, may appear in only one compartment of the model, or, as is the case of blood, it may be the key constituent in a sequence of compartments. Dynamics in each compartment is specified by space-averaged functions of time for pressure and fluid

*Department of Mathematical Sciences, University of Montana, Missoula, MT, 59812, USA.

†Department of Mathematics and Statistics, University of Vermont, 16 Colchester Avenue, Burlington, VT, 05401-1455, USA. Phone: (802) 656-8541, Fax: (802) 656-2552, Email: lakin@emba.uvm.edu

discharge, while incremental changes in flows and volume are obtained by associating resistance and compliance parameters with adjacent compartments. In particular, interaction between adjacent subunits is assumed to take place at the interfaces of the model's compartments. For example, an increase in the volume of one compartment (with a corresponding decrease in the volume of an adjacent compartment) is accounted for by the volume of a 'cup' formed by the deformed membrane at the interface of the two compartments.

It is important to recognize that, in the present context, a compartment denotes a lumped subunit of the mathematical model, and this model subunit does not necessarily correspond to a fixed physical location within the cranial vault (or elsewhere in the body). For example, the cerebrospinal fluid (CSF) space within the skull may be contained in a single subunit governed by a single differential equation. In this case, CSF in the ventricles will not be distinguished from CSF in the subarachnoid space. Rather, both physical regions of intracranial CSF space are represented by the same space-averaged or "lumped" variables. Pressures in other model compartments are similarly space-averaged, but remain fully dynamic functions of time.

Lumped-parameter models of the present type have a long history, dating to the earliest such model of the intracranial system formulated by Monro [18] in 1783. This first model considered incompressible brain matter and blood as its two subunits. In the work of Kellie [11] 40 years later, the vascular component was further subdivided into arterial and venous blood to produce a three-compartment model. Modern work on this type of model has seen a steady increase in the number of fluid compartments, the introduction of a separate cerebrospinal fluid compartment, and a relaxation of the treatment of system constituents as incompressible fluids and brain matter [1, 16, 9, 15, 3]. The model described by Karni *et al.* [10] and elaborated by Sorek *et al.* [21], has seven intracranial compartments, nine resistance and five compliance parameters, as well as a forcing term due to flow input from the heart pump and flow output on the venous side to the jugular veins.

Almost all previous studies of intracranial pressure dynamics have considered the intracranial system to be confined within the nearly-rigid intracranial vault. Connections to whole-body physiology have been indirect, entering, as in [10, 21], mainly through vascular forcing terms in the model. This closed system assumption, known as the Kellie-Monro doctrine, imposes an additional constraint, introduces redundancy into the model's differential equations, and leads to singular behavior for the compliance and resistance matrices. Work by Lakin *et al.* [13] has eliminated this redundancy and provided an exact solution in the linear case where all compliances and resistance parameters are constants. In the nonlinear case with a variable compliance introduced between the brain matter and CSF compartments, a logistic form for this compliance has been shown to allow for large ventricular volume changes without requiring large pressure increases and is effective in determining the etiology of the Alzheimer-like condition Normal Pressure Hydrocephalus as well as the response of this condition to shunting [19]. Predictions of the nonlinear model with the variable compliance have

also been validated by comparison with clinical CSF bolus data measured in a rabbit model [14].

A mathematical model of the present type which, through inclusion of a compliance for CSF storage within the lumbar channel, does not invoke the Kellie-Monro doctrine has been formulated by Czosnyka *et al.*. This model contains three compliances, four resistances, and involves differential equations based on a hydrodynamic model for the physical system and its electrical circuit equivalent. It allows the dynamic relationship between cerebral perfusion pressure, intracranial pressure, and cerebral blood flow in various states of autoregulation to be studied [4]. Use of this model in conjunction with clinical data [5] has determined which of the indices that can be derived using transcranial Doppler ultrasonography and trends of intracranial pressure and blood pressure are useful in clinical tests of autoregulatory reserve.

A key feature in the success of the models in [19, 14, 4, 5] is the use of variable local compliances. Constant local compliances can be consistently used in modeling intracranial pressure dynamics only over very limited ranges of compartment pressure variations. Variable local compliances in lumped-parameter models are therefore essential to realistically predict intracranial pressure dynamics. However, the relationship between local compliances in the mathematical model and the clinical bulk compliance of the entire intracranial system (including “whole-body” components in the lumbar space) has not been previously determined.

Lakin and Gross [12] have shown that the bulk compliance of the entire intracranial system can be related to the slope of the global pressure-volume relationship. This relationship is a curve which describes the changes in CSF pressure that result from adding (or subtracting) incremental changes in CSF volume. The experimentally-measured bulk intracranial pressure-volume relationship for the entire intracranial system determined by Sullivan and Allison [22] using infusion techniques is shown in Fig 1. Since intracranial pressures differ widely between individuals, Sullivan and Allison [22] have developed the concept of “resting pressure” to provide a common reference point for their pressure-volume relationship. Resting pressure is defined to be the CSF pressure at which CSF production is exactly balanced by CSF absorption. In Fig 1, this is the non-zero value of the CSF pressure when no volume change has been induced.

Physiologically, pressure-volume buffering occurs primarily between the CSF and vascular components of body. At lower pressures, this buffering is associated with the lower pressure plateau in Fig 1 in the neighborhood of resting pressure. On this lower plateau, the CSF system has a high compliance. Changes in CSF volume are easily compensated for by slight expansions or contractions of the venous system. Consequently, a small volume change in this lower pressure regime will produce only a small change in intracranial pressure (ICP). It is worth explicitly noting that in this pressure range, significant compensation is provided by the buffering action of the spinal theca, which lies outside of the cranial vault and hence outside of the closed-system (Kellie-Monro doctrine) models for intracranial pressure dynamics. Moving

upward onto the steepening portion of the pressure-volume curve in Fig 1, compensation for larger increases in volume continues to be accomplished through expulsion of blood from the venous system. However, as CSF volume increases, it now becomes increasingly difficult to expel additional venous blood. Consequently, the steepness of the pressure-volume curve increases, compliance of the CSF system decreases, and small volume changes now produce increasingly large relative changes in ICP. Above the 30 to 40 mmHg range, and in particular as the pressures approach the diastolic blood pressure, intracranial pressures are sufficiently high that interarterial blood volume can be affected. With the introduction of this additional means of compensation for added CSF volume, the pressure-volume curve becomes less steep at higher pressures, changes concavity, and smoothly goes to the upper pressure plateau at diastolic pressures. Compliances now increase and are again large on the upper pressure plateau. Consequently, on the upper pressure plateau, small volume additions will again produce only small pressure changes. Beyond the upper pressure plateau at systolic pressure, the intracranial system contains no additional compensatory features to buffer additional volume increases, so the pressure-volume curve rises steeply and the compliance of the CSF system falls to zero.

The aim of the present work is to determine physiologically-motivated local compliances in a compartmental model with “whole-body” physiology so that simulations of CSF infusion with this mathematical model recover the experimentally-determined pressure-volume relationship over the full range of intracranial pressures. This will be the first time that this global pressure-volume relationship has been accurately predicted by a mathematical model for intracranial pressure dynamics. A consistent link between variable local compliances and the experimentally-measured global pressure-volume relationship is essential if lumped-parameter models are to be capable of realistically predicting intracranial pressure dynamics.

2 THE MODEL

In order to mathematically describe the dynamics of CSF production, absorption, and storage without introducing excessive complexity, the simplified four compartment lumped-parameter model shown in Fig 2 will be used. In this particular model, the CSF space is defined as a single compartment with a spatially-averaged pressure P_f . The intracranial space is further divided into two vascular compartments; artery and vein, with pressures; P_a and P_v respectively. Finally, the rest of the body makes up the fourth compartment. It is from here that all fluid flow into the intracranial region originates and into which all intracranial drainage is absorbed. This compartment contains the spinal theca, the lumbar portion of CSF space which provides a high proportion of the initial buffering on the lower pressure plateau of the experimentally-measured pressure-volume relationship [22]. Due to the similarities between this compartment

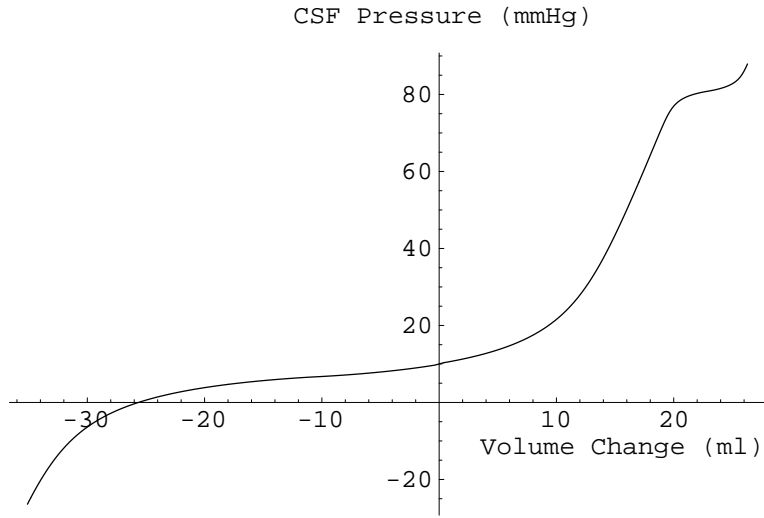


Fig. 1. The clinically observed CSF pressure-volume relationship. The curve crosses the vertical axis at a non-zero 'resting' pressure.

and the ground node in an electrical circuit, this compartment is labeled “ground” with a known pressure P_g .

The resistance to flow through the arteries is lumped at the artery-vein interface (R_{av}), and similarly the resistance to flow through the veins is lumped at the outflow of the vein compartment (R_{vg}). Because the CSF production rate is known to remain nearly constant throughout a wide range of intracranial pressures [2, 8, 22], Q_f is considered a constant flow originating from the arterial side of the vasculature. It should be noted that Q_f is not a flow of blood into the CSF space, but rather a flow in the form of secreted CSF from capillary like structures known as choroid plexuses. Conversely, the absorption rate of CSF is pressure driven [2, 8, 22], and the resistance to this flow is lumped at the CSF-vein interface (R_{fv}). Because arterial blood supply to the brain is known to be well auto-regulated, the flow Q_A is considered constant. In order to simulate clinical infusion tests, an infusion term (Q_{inf}) is included to allow an infusion of mock CSF into the CSF compartment.

In this model, there are three “local” compliances relating the pressure differences between adjacent compartments to volume adjustments. C_{af} represents the compliance between the arteries and CSF, while C_{fv} represents the compliance between the CSF and intracranial veins. C_{fg} represents the ability of the spinal portion of CSF space to expand by compressing the large veins that surround the spinal theca outside of the cranial vault. It is usually through the spinal theca, which communicates with the subarachnoid CSF space, that researchers safely infuse or withdraw fluid into, or out of, the CSF space.

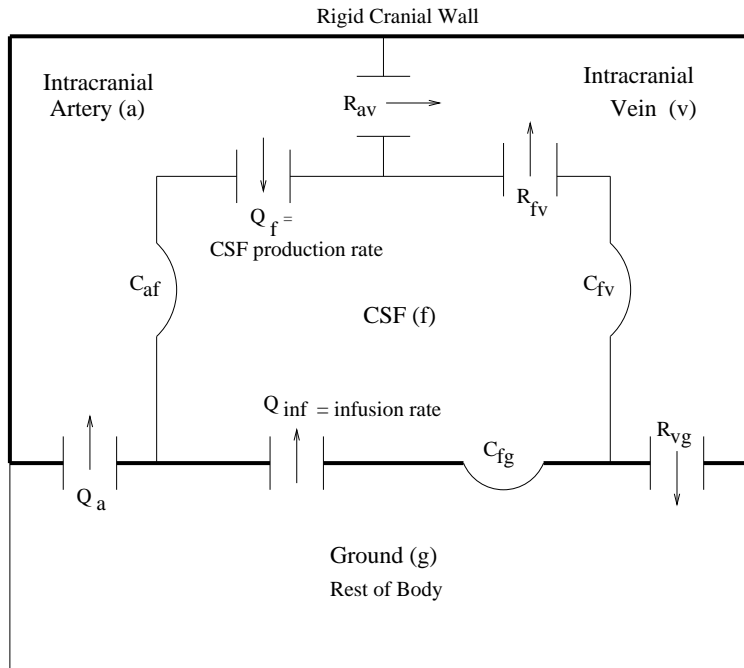


Fig. 2. The Four Compartment model

Even though the focus in the present work is on CSF-vascular pressure buffering, it may seem questionable that the brain is not considered as a compartment in this simplified intracranial pressure model. However, due to the large resistances associated with the blood-brain and CSF-brain barriers, the flow into and out of the interstitial brain tissue is several orders of magnitude less than the smallest fluid flow considered in the four-compartment model. Therefore, brain volume is considered constant during the simulated infusion tests and any deformation of the brain is compensated for by an equal composite of deformations in one or more of the included compartments. For example, a CSF volume increase may deform the shape of the brain, but the intracranial fluid compensation must be in the form of expelled blood or the expansion of the CSF space in the rest of the body.

3 DERIVATION

Three basic assumptions lead to the equations describing the dynamics of this system:

- All fluids are considered incompressible and isothermal.
- Pressure driven flows are laminar and related to pressure differences by

$$Q_{ij} = \frac{P_i - P_j}{R_{ij}} = Z_{ij}(P_i - P_j) = Z_{ij}P_{ij}, \quad (1)$$

where Q_{ij} is the flow from compartment i into compartment j , P_i and P_j are the spatially-averaged pressures of compartments i and j , R_{ij} is the lumped resistance to flow between compartments i and j , $R_{ij} = -R_{ji}$, the fluidity Z_{ij} is the inverse of resistance R_{ij} , and $P_{ij} = P_i - P_j$ is the pressure difference between the two compartments.

- The deformation of the membrane between adjacent compartments is a function of the change in pressure difference between these compartments;

$$\frac{dV_{ij}}{dt} = C_{ij} \frac{d(P_i - P_j)}{dt} = C_{ij} \frac{d(P_{ij})}{dt}, \quad (2)$$

where V_{ij} denotes the instantaneous volume of the ‘cup’ formed at the interface of compartments i and j , C_{ij} denotes the compliance between these two compartments, and $C_{ij} = C_{ji}$.

It should be noted that these assumptions are analogous to those in electrical circuit analysis, where each compartment represents a node, and pressure and flow are analogous to voltage and current. In this analogy, equation (1) describes the current across a resistor and equation (2) describes the change in charge on a capacitor. Consequently, the governing system of differential equations for the model in Fig 2 are very similar to those describing an RC circuit.

Invoking the conservation of mass in each intracranial compartment, or alternatively applying Kirchoff’s current law at each node, results in three differential equations;

$$Q_a - Q_f - Z_{av}P_{av} = C_{af}\dot{P}_{af}, \quad (3)$$

$$Q_f + Q_{inf} - Z_{fv}P_{fv} = C_{af}\dot{P}_{fa} + C_{fv}\dot{P}_{fv} + C_{fg}\dot{P}_{fg}, \quad (4)$$

$$Z_{av}P_{av} + Z_{fv}P_{fv} - Z_{vg}P_{vg} = C_{fv}\dot{P}_{vf}. \quad (5)$$

Replacing equation (4) with the sum of equations (3), (4) and (5), setting

$$P_{av} = P_{af} + P_{fv},$$

$$P_{vg} = P_{fg} - P_{fv},$$

and formulating the resulting differential equations in matrix form now yields

$$\mathbf{C}\dot{\mathbf{P}} + \mathbf{Z}\mathbf{P} = \mathbf{Q} \quad (6)$$

with

$$\mathbf{C} = \begin{pmatrix} C_{af} & 0 & 0 \\ 0 & C_{fv} & 0 \\ 0 & 0 & C_{fg} \end{pmatrix} \quad \mathbf{Z} = \begin{pmatrix} Z_{av} & Z_{av} & 0 \\ Z_{av} & Z_{av} + Z_{fv} + Z_{vg} & -Z_{vg} \\ 0 & -Z_{vg} & Z_{vg} \end{pmatrix}$$

$$\mathbf{P} = \begin{pmatrix} P_{af} \\ P_{fv} \\ P_{fg} \end{pmatrix} \quad \mathbf{Q} = \begin{pmatrix} Q_a - Q_f \\ 0 \\ Q_a + Q_{inf} \end{pmatrix}.$$

Equation (6) is an ordinary matrix differential equation, where the dot represents differentiation with respect to time.

Conversion from the pressure difference vector (\mathbf{P}) into non-difference form is easily accomplished through the linear transformation

$$\Phi = \mathbf{T}\mathbf{P} + \mathbf{P}_g, \quad (7)$$

$$\Phi = \begin{pmatrix} P_a \\ P_f \\ P_v \end{pmatrix} \quad \mathbf{T} = \begin{pmatrix} 1 & 0 & 1 \\ 0 & 0 & 1 \\ 0 & -1 & 1 \end{pmatrix} \quad \mathbf{P}_g = \begin{pmatrix} P_g \\ P_g \\ P_g \end{pmatrix}.$$

In accordance with the electrical circuit analogy, P_g will be assigned the value zero throughout the rest of this analysis. While this value does not necessarily reflect the spatially-averaged pressure of the rest of the body, this compartment merely functions as a large source and drainage space for the intracranial fluids. Further, scale values for the model's resistances, which are derived using mean pressure differences, will be calculated in such a way that intracranial pressures are indeed indicative of human physiology and no translation of the solution vector by \mathbf{P}_g is necessary.

4 PARAMETER SCALE VALUES

Before simulating infusion tests on the model, appropriate scale values for the problem parameters such as resting pressures and flows, resistances (or fluidities), and compliances must be calculated from available data. In this section, we focus on calculating the model's constant fluidities and resting pressures as this can be achieved without assigning values to the compliance terms. Throughout this preliminary analysis, pressures and flows are given mean values in the sense that time-dependent oscillations

about these mean values are disregarded. To use clinical studies, this requires some form of averaging data over each period.

Solving equation (1) for each fluidity in terms of pressure-difference and flow yields

$$Z_{av} = (Q_a - Q_f)/(\bar{P}_a - \bar{P}_v), \quad (8)$$

$$Z_{fv} = Q_f/(\bar{P}_f - \bar{P}_v), \quad (9)$$

$$Z_{vg} = Q_a/(\bar{P}_v - \bar{P}_g), \quad (10)$$

where an overbar indicates resting pressure before the start of an infusion test. Unfortunately, not all of the quantities on the right hand side of these equations are known from the outset. In particular, \bar{P}_v is often not measured by clinical researchers. However, \bar{P}_v may be calculated in such a way that the model behaves properly in terms of CSF absorption as a function of CSF pressure change. This functional relationship is described next.

In clinical procedures regarding the CSF pressure-volume relationship, preliminary steady-state infusion tests are generally performed in order to obtain the formation and absorption rates of CSF at different CSF pressures. These tests vary in technique but usually involve adding or withdrawing fluid from the CSF space at a constant rate. Adequate time is allowed for the CSF pressure to reach a steady state, and estimations of CSF production and absorption can be then made at that particular CSF steady-state pressure. For a more detailed description of these types of tests, see [2, 7, 22].

In general, the CSF production rate remains almost constant at Q_f over an extensive range of pressures, and clinical data indicates that the CSF absorption rate is linearly related to CSF pressure increases by

$$\mathcal{A} = \mathcal{Z}(P_f^* - \bar{P}_f) + Q_f. \quad (11)$$

Here, \mathcal{A} is the absorption rate, in ml/min, at the steady-state pressure P_f^* and \mathcal{Z} is the conductance of CSF outflow. It should be noted that the conductance \mathcal{Z} of CSF outflow and the fluidity Z_{ij} are both measured in units of (ml/min)/(mmHg). However, \mathcal{Z} represents the slope of the linear relationship between CSF absorption and CSF pressure increase. By contrast, Z_{ij} is the slope of the assumed linear relationship in equation (1) between intercompartmental flow and intercompartmental pressure differences. Therefore, \mathcal{Z} is not explicitly included as a model parameter, but is instead used as a clinically observed reference value from which an estimation of \bar{P}_v will be made. For a complete description of how the conductance of CSF outflow is calculated and the results for healthy human subjects, see Albeck *et al.* [2].

Simulating this type of infusion test on the model requires a nonzero Q_{inf} in equation (6). However, this term can be considered sufficiently small that the linear approximation for all pressure dependent compliances remains valid. In this linear

case, with all resistances and compliances constant, the solution of equation (6) tends to the steady state (\mathbf{P}^*) defined by

$$\mathbf{P}^* = \mathbf{Z}^{-1}\mathbf{Q}. \quad (12)$$

In the case of zero infusion, equation (12) reduces to the form

$$\bar{\mathbf{P}} = \mathbf{Z}^{-1}\bar{\mathbf{Q}}, \quad (13)$$

where

$$\bar{\mathbf{Q}} = [Q_a - Q_f, 0, Q_a]^{tr}.$$

Here, $\bar{\mathbf{P}}$ indicates the initial resting condition prior to the start of an infusion test, and the superscript *tr* denotes vector transposition. Subtracting (13) from (12) results in

$$\mathbf{P}^* - \bar{\mathbf{P}} = \mathbf{Z}^{-1}(\mathbf{Q} - \bar{\mathbf{Q}}) = \mathbf{Z}^{-1}\mathbf{Q}_i \quad (14)$$

where

$$\mathbf{Q}_i = [0, 0, Q_{inf}]^{tr}.$$

Therefore, transforming back to non-difference form using equation (7) yields

$$P_f^* - \bar{P}_f = [\mathbf{T}\mathbf{Z}^{-1}]_{(2,3)} Q_{inf} = \left(\frac{1}{Z_{fv}} + \frac{1}{Z_{vg}}\right) Q_{inf}, \quad (15)$$

where \mathbf{T} is defined in equation (7), and $[\mathbf{T}\mathbf{Z}^{-1}]_{(2,3)}$ is the second element in the third column of $\mathbf{T}\mathbf{Z}^{-1}$. This term is simplified on the right hand side of equation (15).

As in the clinical experiments, the model steady state is achieved when the CSF absorption rate equals the sum of the CSF infusion and production rates

$$\mathcal{A} = Q_{inf} + Q_f \quad (16)$$

$$= \left(\frac{1}{Z_{fv}} + \frac{1}{Z_{vg}}\right)^{-1} (P_f^* - \bar{P}_f) + Q_f. \quad (17)$$

Equation (17) is a result of solving equation (15) for Q_{inf} and substituting this into equation (16).

As can be seen from equation (17), the model absorption rate is indeed linear in CSF pressure increase. Therefore it will be required *a priori* that this linear relationship agrees with that determined clinically, i.e.

$$\left(\frac{1}{Z_{fv}} + \frac{1}{Z_{vg}}\right)^{-1} = \mathcal{Z}. \quad (18)$$

At this point, all of the terms on the right hand side of equations (8)-(10) may be considered known, with the exception of \bar{P}_v . However, this mean pressure value can

be calculated by substituting equations (9) and (10) into equation (18) and solving for \overline{P}_v , which results in

$$\overline{P}_v = \frac{\frac{Q_a Q_f}{Z} + \overline{P}_g Q_f - \overline{P}_f Q_a}{Q_f - Q_a}. \quad (19)$$

In order to perform numerical simulations on the model, specific numerical scale values must be assigned for the mean pressures and fluidity parameters. This is done with respect to the physiologically normal adult human and results in the list below. It should be kept in mind that the sources for the following parameters generally give a range of values and the scale value chosen below lies within this range.

- $\overline{P}_a = 80$ mmHg (resting intracranial artery pressure)
This is primarily based on the CSF upper pressure plateau occurring near diastolic blood pressure [22]. Further, spatial averaging of intracranial arterial pressure will result in a value less than the 100 mean mmHg arterial pressure associated with the infraclavicular arteries [8].
- $\overline{P}_f = 10$ mmHg (resting CSF pressure)
Sources vary and cite values of 10 mmHg [8, 22, 10, 21], 11 mmHg [2], and 11.25 mmHg [7].
- $Q_a = 750$ ml/min (mean arterial input)
Sources agree on this value [8, 10, 21].
- $Q_f = 0.35$ ml/min (CSF production rate)
Sources vary and cite values of 0.3 ml/min [10, 21], 0.35 ml/min [8], 0.4 ml/min [2], and 0.43 ml/min [7].
- $Z = 0.11$ (ml/min)/mmHg (Conductance of CSF outflow)
Sources vary and cite values ≥ 0.10 (ml/min)/mmHg [22], 0.18 (ml/min)/mmHg [7], and 0.11 (ml/min)/mmHg [2] for healthy human subjects.

The following parameters are then calculated from the above values as:

- $\overline{P}_v = 6.82137$ mmHg (resting intracranial vein pressure) eq (19).
- $Z_{av} = 10.2441$ (ml/min)/mmHg (artery-vein fluidity) eq (8).
- $Z_{fv} = 0.11011$ (ml/min)/mmHg (CSF-vein fluidity) eq (9).
- $Z_{vg} = 109.949$ (ml/min)/mmHg (vein-ground fluidity) eq (10).

Since the above estimations are based on varying clinical data and certain physiological assumptions, a sensitivity analysis was performed on the steady-state solutions of the linearized problem. Because of the relatively large fluidities between vascular compartments, the solutions for P_a^* and P_v^* are insensitive to all problem

parameters and remain nearly constant at their prescribed mean values during an infusion simulation or under fluidity perturbations. On the other hand, P_f is extremely sensitive to the infusion rate as one would expect. To normalize this result, the ratio $(P_f^* - \bar{P}_f)/Q_{inf}$ was considered the relevant variable when analyzing sensitivity during an infusion simulation. However, by implicitly including \mathcal{Z} as a problem parameter, equations (15) and (18) yield

$$\frac{P_f^* - \bar{P}_f}{Q_{inf}} = \frac{1}{\mathcal{Z}}. \quad (20)$$

Therefore, the increase in CSF pressure per infusion rate is determined exclusively by the prescribed value for \mathcal{Z} . Considering the range of values provided by clinical data, this ratio lies between 5 and 10 mmHg/(ml/min). As an example, if artificial CSF is infused at a constant rate of 5 ml/min, the model predicts the CSF pressure should increase by 25 to 50 mmHg depending on the conductance of CSF outflow, thus reflecting the clinically observed sensitivity of CSF pressure increase to the conductance of CSF outflow. Specifically, If the studies of Friden and Ekstedt [7] are recreated on the model using $\mathcal{Z} = 0.18$ (ml/min)/mmHg and $Q_{inf} = 7.2$ ml/min, the model predicts a CSF pressure increase of 40 mmHg, which is in close agreement with the clinical results (see figure 2 in [7]).

In general, $P_f^* - \bar{P}_f$ is most sensitive to Z_{fv} which, by equation (9), is most sensitive to \bar{P}_v . Furthermore, \bar{P}_v is the parameter for which there is the least clinical data. Overcoming this lack of data provided the motivation for inclusion of the conductance \mathcal{Z} of the CSF outflow in the calculation of \bar{P}_v . With the above formulation, the dynamics of the CSF system will behave in accordance with clinical evidence in the linearized steady-state solution. Furthermore, in the nonlinear case, where compliances are pressure dependent, the solution still tends to the steady state defined by \mathbf{P}^* and the above sensitivity analysis is still valid. The difference is in the shape of the transient solution and the associated volume changes.

In the ideal case, the remaining determinations regarding the local compliances C_{af} , C_{fv} and C_{fg} , would follow from the definition of compliance in equation (2) as

$$C_{ij} = \frac{dV_{ij}}{dP_{ij}}, \quad (21)$$

and clinical data would provide local volume changes associated with changes in pressure differences. Unfortunately, this type of physical data is unavailable. For example, clinical measurements provide CSF pressure increase as a result of a net (global) CSF volume increase, but this data does not differentiate how much of this volume increase is associated with displaced venous blood. Furthermore, this data does not, in general, measure mean arterial or venous pressure changes during such a procedure. Therefore, in reality, local compliance estimations must be based on global CSF data as well as some basic assumptions regarding the behavior of local compliances. The fol-

lowing section deals with an analysis of how these assumptions allow global data to be interpreted locally.

5 SYSTEM COMPLIANCE

In a modeling context, the clinically measured pressure-volume curve for intracranial space depicted in Figure 1 can be interpreted as the pressure-volume relationship for a two-compartment model consisting of the CSF space and the rest of the body. If the rest of the body is again considered to be a ground with zero compartmental pressure, then values for the CSF pressure on the vertical axis in Figure 1 become simply the pressure difference between the model's two compartments. Similarly, the slope of the pressure-volume relationship in Figure 1 is the pressure difference change due to an integrated volume change in the CSF space and is therefore the local elastance between the model's two compartments. If the clinical pressure-volume relationship is inverted, as shown in Figure 3, to give volume changes as a function of CSF pressures, then the slope of this volume-pressure relationship is the local compliance between the CSF and rest of body compartments. This interpretation provides an identification between the measured global compliance and the single local compliance allowed in a two-compartment model. However, what is needed is the relation of the global compliance to the multiple local compliances in models with additional compartments.

5.1 Global Compliance

By plotting the slope of the global volume-pressure relationship at each CSF pressure, the picture of the global CSF compliance given in Fig 4 is obtained. By the interpretation above, this curve is also the single local compliance $C_g(P)$ in a two compartment model. The shape of this curve and the physiology of intracranial pressure buffering described in the Introduction now allow a decomposition of C_g into the three local compliances in the four-compartment model.

On the portion of Fig 4 below CSF pressures of 60 mmHg, buffering is provided by compression of the veins surrounding the spinal theca and the intracranial venous system. Above pressures of 60 mmHg, buffering comes from compression of the arterial vessels. At the transition pressure of 60 mmHg, venous buffering has nearly ceased while arterial buffering has not yet commenced. Therefore, the small value of C_g at this pressure can be interpreted as the background compliance between the CSF space and the ground compartment. Since the pressure ranges for the different physiological buffering mechanisms only overlap to a minimal extent, the local compliance C_g over the full range of pressures can be written as an additive composite of the three local compliances in the four compartment model. The following near equalities will thus hold:

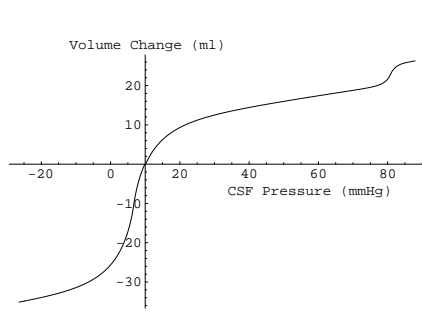


Fig. 3. The clinically observed CSF pressure-volume curve inverted to express CSF volume change as a function of pressure.

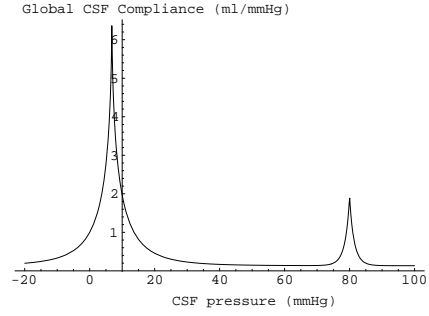


Fig. 4. Global CSF Compliance (C_g) = the slope of the CSF volume-pressure curve.

$$C_g(60) \approx C_{fg}, \quad (22)$$

$$C_g(\bar{P}_v) \approx C_{fg} + C_{fv}(0), \quad (23)$$

$$C_g(\bar{P}_a) \approx C_{fg} + C_{af}(0), \quad (24)$$

$$C_g(\bar{P}_f) \approx C_{fg} + C_{fv}(\bar{P}_{fv}). \quad (25)$$

If the above four relations are taken as strict equalities, three additional constraints are necessary to fully determine the local compliances.

5.2 Local Compliance

In order to illustrate the behavior of a local compliance that is dependent upon pressure differences, consider an elastic membrane separating two fluids in a rigid tank as seen in Fig 5. The compliance of this system can be considered a measurement of the membrane elasticity. On physiological grounds, when the pressures in compartment A and B are the same (a pressure difference of zero), the membrane will be most elastic. As the pressure difference between A and B increases in either direction, the membrane will stretch in the opposite direction to the pressure gradient causing the compliance to diminish. Three possible graphical depictions of this type of relationship are seen in Fig 6. The non-differentiable curve shown with a solid line is most similar to one of the individual peaks in Fig 4. However, in all three curves, the pressure-difference dependent compliance has a maximum at a pressure difference of zero and diminishes as the pressure difference increases in either direction. Clinical evidence suggests a symmetric compliance, as shown in the global p/C graphs depicted in figures 6 - 8 of Friden and Ekstedt [7]. In addition, the symmetry is consistent with the assumption in the model that, for local compliances, $C_{ij} = C_{ji}$.

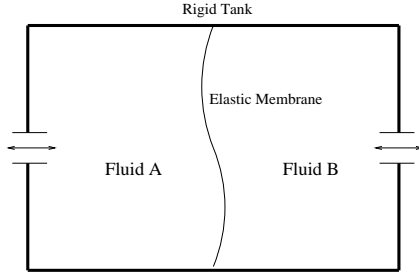


Fig. 5. Two fluid filled compartments separated by an elastic membrane.

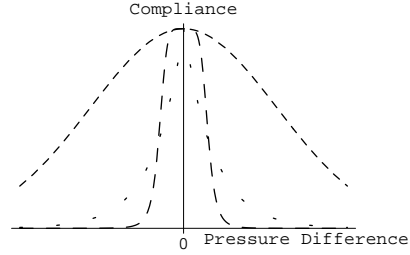


Fig. 6. Possible shapes for a local pressure-difference dependent compliance.

In the four-compartment model, the local compliances C_{af} and C_{fv} will be based on the assumptions given above. C_{af} will be a function of $P_a - P_f = P_{af}$ and C_{fv} will be a function of P_{fv} . The compliance C_{fg} is considered constant as this parameter reflects a general buffering mechanism for CSF expansion in the absence of either of the other local compliances. In addition, within the context of the current volume adjustments, the ability of the rest of the body to expand or contract is considered unlimited. A more realistic C_{fg} might be one that diminishes slightly as CSF pressure increases. However, for the present purposes, the two variable compliances C_{af} and C_{fv} will suffice to capture the general shape of the CSF pressure-volume relationship and the effect of a slightly diminishing C_{fg} would be negligible.

All three of the shapes displayed in Fig 6 were employed in simulated infusion tests but, as might be expected, only the non-differentiable curve (denoted by the solid line) resulted in realistic CSF pressure-volume curves. The upper dashed curve required excessive volume changes to induce recorded pressure changes. The middle dashed curve resulted in a pressure volume curve that was piecewise linear. This is not in agreement with clinical results. Therefore, throughout the remainder of this analysis, variable compliances will have the shape described by the solid line in Fig 6.

Therefore, local compliances will have a shape defined by

$$C_{ij}(P_{ij}) = C_{ij}^o \exp^{-r_{ij}|P_{ij}|^{\alpha_{ij}}}, \quad (26)$$

where r_{ij} and α_{ij} are positive, and $C_{ij}^o = C_{ij}(0)$. If the value of this compliance is known at resting pressure \bar{P}_{ij} and denoted by \bar{C}_{ij} the following relationship between α_{ij} and r_{ij} must hold:

$$r_{ij}|\bar{P}_{ij}|^{\alpha_{ij}} = -\ln(\bar{C}_{ij}/C_{ij}^o). \quad (27)$$

Since C_{ij}^o is the maximum value of the compliance, $\ln(\bar{C}_{ij}/C_{ij}^o)$ will be less than zero and r_{ij} is positive by equation (27).

Considering the above equations, each of the pressure-difference dependent compliances ($C_{af}(P_{af})$ and $C_{fv}(P_{fv})$) requires three parameter evaluations; C_{ij}^o , r_{ij} and

α_{ij} , and the constant compliance (C_{fg}) requires one. Thus, in order to fully calibrate the local compliances, a total of seven constraints are necessary. Four of these constraints are given above by considering C_g to be a composite of C_{fg} , C_{af} , and C_{fv} .

The remaining three constraints must be obtained using further data regarding the global CSF pressure-volume relationship. This can be done by either numerically solving for the parameters involved in each local compliance from data similar to equations (22) - (25), or simulating infusion tests and applying a shooting method to these parameters. Both of these methods were attempted and the former proved to be adequate due to artery and venous pressures remaining nearly constant during simulated infusion tests.

Calculations using clinical data from [7, 22] now result in the pressure-difference dependent compliances depicted in Figures 7 and 8. C_{fg} was calibrated at a constant value of 0.1333 ml/mmHg

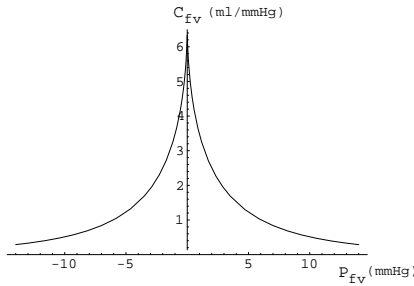


Fig. 7. The local, pressure-difference dependent compliance $C_{fv}(P_{fv})$.

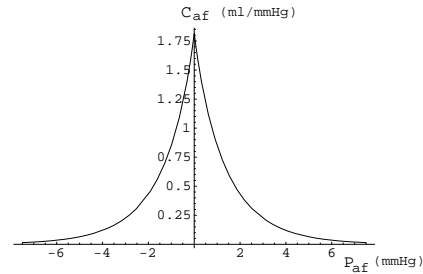


Fig. 8. The local, pressure-difference dependent compliance $C_{af}(P_{af})$.

6 INFUSION SIMULATIONS

All of the relevant parameters in the lumped-parameter model are now fully calibrated and infusion simulations may be performed on the model. Using the fluidity calibrations described in section 4 and the compliance calibrations described in section 5.2, equation (6) may now be solved for various infusion rates. Equation (6) was numerically solved using the symbolic mathematical software package *Mathematica* employing maximum accuracy settings. The solution for P_f may then be taken as the second term in Φ from equation (7). The integrated CSF volume change may be calculated as

$$V_f(t) = \int_0^t Q_{inf} + Q_f - Z_{fv} P_{fv}(\tau) \, d\tau, \quad (28)$$

which was also calculated numerically using *Mathematica*.

Performing this simulation for a sequence of CSF infusions and withdrawals results in the four-compartment model with three local compliances predicting the global CSF pressure-volume curve depicted in Fig 9.

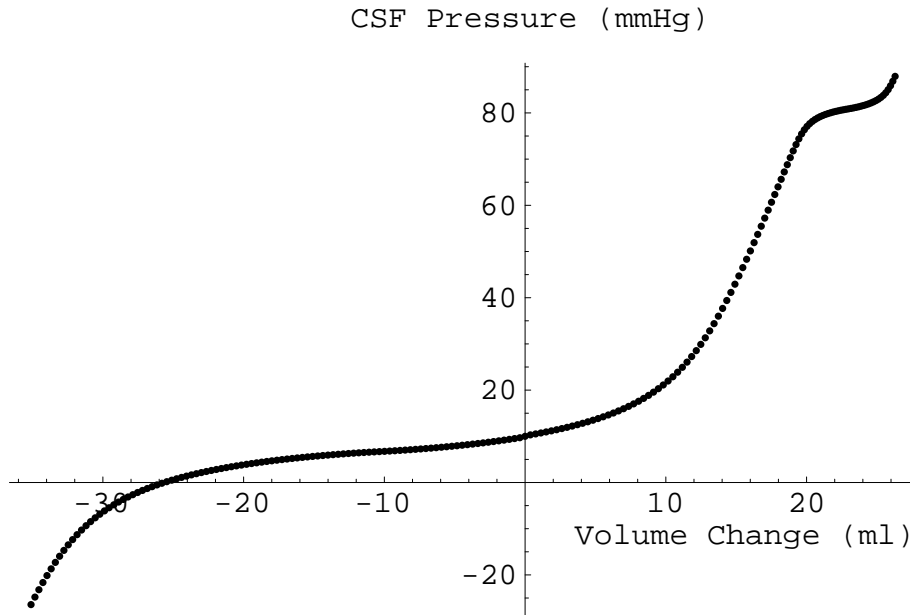


Fig. 9. The global CSF pressure-volume curve predicted by simulated infusion tests.

As can be seen by comparing Fig 1 with Fig 9, the inclusion of two pressure-difference dependent local compliances (C_{fv} and C_{af}) results in a predicted pressure-volume curve that captures all of the relevant aspects of the clinically observed relationship including both pressure plateaus, the change in concavity between the plateaus, and the loss of all compliance above diastolic pressure. It should be noted that different infusion rates were implemented and the shape of this curve was invariant. In addition, when an infusion was stopped, CSF pressure and volume returned to their resting values along the same curve.

7 CONCLUSIONS

Previous mathematical considerations of the clinically-determined global pressure-volume relationship in Fig 1 have involved only a formulation of various fits for the

actual curve itself. It has been known for some time that this curve can be reasonably well represented by an exponential function over much of the normal pressure range. However, exponential fits depart markedly from the clinical results at higher pressures. Even at lower pressures, if the relationship between CSF volume and pressure were truly exponential then a semi-logarithmic plot of CSF pressure versus volume would be a straight line, implying that the so-called Pressure-Volume Index is a constant. As noted in [7], this clearly is not the case. Attempts to modify the exponential model, which include adding a constant as an inhomogeneous term in the differential equation for dP/dV , have not resolved this problem. By contrast, a logistic model of the pressure-volume relationship [12] has been shown to provide a robust fit from low pressures through the upper pressure plateau. However, even here, the vertical asymptote at systolic pressure where all compliance is lost is not represented in the logistic model.

This work represents the first successful formulation that recovers the global clinical pressure-volume relationship directly from simulated infusion tests using a mathematical model. The variable local compliance parameters in this four-compartment compartmental model are appropriate non-differentiable functions of pressure differences whose forms are motivated by the physiology of pressure buffering at various CSF pressure levels. Because CSF-venous and CSF-arterial pressure buffering mechanisms are operative in nearly non-overlapping CSF pressure ranges, the global intracranial compliance, interpreted as the single local compliance in a two-compartment model, can be related to the local compliances in the four-compartment model as an additive composite function. This work should provide the basis for deriving variable local compliance parameters in more involved compartmental models for intracranial pressure dynamics which include multiple compartments for the CSF, arterial, and venous spaces.

ACKNOWLEDGEMENTS

Portions of this work were supported by the National Science Foundation under grant number DMS-96-26391 and by NASA under grant numbers NGT-40054 and NCC5-394. This research was done while the first author was in residence at the University of Vermont.

REFERENCES

1. Agarwal, G.C.: Fluid flow-a special case. *Biomedical engineering*, (1971), (Brown, J.H.V., Jacobs, J.E. and Stark L. eds), F.A.Davis Company, Philadelphia.
2. Albeck, M.J., Gjerris, F. and Sorenson, P.S.: Intracranial pressure and cerebrospinal fluid outflow conductance in healthy subjects. *J. Neurosurgery*, 74 (1991), pp. 597-600.
3. Chopp, M. and Portney, H.D.: Systems analysis of intracranial pressure. *J. Neurosurg.*, 53 (1980), pp. 516-527.

4. Czosnyka, M., Piechnik, S., Koszewski, W., Laniewski, P., Maksymowicz, W., Paluszek, K., Smielewski, P., Zabolotny, W. and Zaworski, W.: The dynamics of cerebral blood perfusion pressure and CSF circulation – a modelling study. *Intracranial Pressures VIII*, Avezaat, C.J.J. *et al.* (eds). Springer, Berlin - Heidelberg, 1993, pp 699–706.
5. Czosnyka, M., Piechnik, S., Richards, H.K., Kirkpatrick, P., Smielewski, P. and Pickard, J.D.: Contribution of mathematical modelling to the interpretation of bedside tests of cerebrovascular autoregulation. *J. Neurol. Neurosurg. Psychiatry*, 63 (1997), pp 721–731.
6. Davson, H., Hollingsworth, B. and Segal, M.B.: The mechanism of drainage of the cerebrospinal fluid. *Brain*, 93 (1970), pp. 665–678.
7. Friden, H. and Ekstedt, J.: Volume/Pressure relationships of the cerebrospinal space in humans. *J. Neurosurgery*, 4 (1983), pp. 351–366.
8. Guyton, A.C.: *Textbook of Medical Physiology* (second edition). W.B. Saunders Company, Philadelphia, 1991.
9. Hakim, S.V., Venegas, J.G. and Burton, J.D.: The physics of the cranial cavity, hydrocephalus and normal pressure: mechanical interpretation and mathematical models. *Surg. Neurol.*, 5 (1976), pp. 187–210.
10. Karni, Z., Bear, J., Sorek, S. and Pinczewski, Z.: A quasi-steady state compartmental model of intracranial fluid dynamics. *Med. Biol. Engng. Comput.*, 25 (1987), pp. 167–172.
11. Kellie, G.: An account ..., with some reflections on the pathology of the brain. *Edinburgh Med. Chir. Soc. Trans.*, 1 (1824), pp. 84–169.
12. Lakin, W.D. and Gross, C.E.: A hemodynamic model for the arterial pulsatile contribution to the intracranial pressure wave. *Neurol. Res.*, 14 (1992), pp. 219–225.
13. Lakin, W.D., Yu, J. and Penar, P.L.: Mathematical modeling of pressure dynamics in the intracranial system. *Nova Journal of Mathematics, Game Theory and Algebra*, 5-2 (1996).
14. Lakin, W.D., Yu, J., and Penar, P.L.: Analysis and Validation of a Mathematical Model for Intracranial Pressure Dynamics. *Math. and Computer Modelling of Dynamical Systems*, 3 (1999), pp. 54–73.
15. Lewer, A.K. and Bunt, E.A.: Dysfunction of the fluid mechanical craniospinal systems as revealed by stress/strain diagrams. *S. Afr. Mech. Engng*, 28 (1978), pp. 159–166.
16. Marmarou, A., Shulman, K. and LaMorges, J.: Compartmental analysis of compliance and outflow resistance of the cerebrospinal fluid system. *J. Neurosurg.*, 43 (1975), pp. 523–534.
17. Miller, J.D.: Volume and pressure in the craniospinal axis. *Clin. Neurosurg.*, 22 (1975), pp. 76–105.
18. Monro, J.: *Observations on the Structure and Functions of the Nervous System*. W. Creech, Edinburgh, 1783.
19. Penar, P., Lakin, W.D., and Yu, J.: Normal Pressure Hydrocephalus: An Analysis of Etiology and Response to Shunting Based on Mathematical Modeling. *Neurological Research*, 17 (1995), pp. 83–88.
20. Portney, H.D. and Chopp, M.: Intracranial fluid dynamics, interrelationship of CSF and vascular phenomenon. *Concepts in Pediatric Neurosurgery*, 3 (1983), pp. 133–144.
21. Sorek, S., Bear, J. and Karni, Z.: A non-steady compartmental flow model of the cerebrovascular system. *J. Biomechanics*, 21 (1988), pp. 695–704.
22. Sullivan, H. and Allison, J.: Physiology of cerebrospinal fluid. *Neurosurgery*, 3 (1985), pp 2125–2135. (R. Wilkins and S. Rengachary eds), McGraw Hillbook Co., New York.